*Can. J. Remote Sensing*, Vol. 33, No. 4, pp. 250–259, 2007

# Effects of band combinations and GIS masking on fire-scar mapping at local scales in east-central Florida, USA

Guofan Shao and Brean W. Duncan

**Abstract.** The fire-adapted vegetation in east-central Florida provides habitat for many threatened and endangered species, such as the Florida scrub-jay (*Aphelocoma coerulescens*). Accurate fire occurrence records are critically important for better understanding the relationship between fire and vegetation structure. The rapid growth rates of fire-adapted vegetation in east-central Florida make it difficult to capture detailed fire scars with remote sensing data acquired weeks after the fires. The objective of this study is to develop a reliable remote sensing approach for accurately mapping burned areas in Florida scrub vegetation at the National Aeronautics and Space Administration (NASA) John F. Kennedy Space Center (KSC) and Merritt Island National Wildlife Refuge (MINWR). Landsat thematic mapper (TM) data acquired on 21 April 1987 were used for classification experiments. Geographic information system (GIS) data layers of fire management units (FMUs) with known fire occurrence (presence or absence) were used to mask the original remote sensing data or thematic maps following classification. A separation index (SI) was used to evaluate each individual band for its power to discriminate unburned and burned areas. Twelve classifications with selected band groups derived from Landsat TM data with different geographic extents were compared using an error matrix method. The classification of the four most suitable bands derived for the entire KSC–MINWR area resulted in the highest accuracy. The final map product was generated by overlaying the classified map with the FMU data layer and masking out FMUs that did not burn. This paper addresses a number of issues relevant to the classification of burned areas and includes the effect of geographic extent (GE effect) of remote sensing data on classification, determining the best bands for classification, and cleaning classification results using GIS masking. It also serves as the first published effort to map fire scars in the Florida scrub and flatwoods vegetative communities of the southeastern US using image processing techniques.

**Résumé.** La végétation adaptée aux incendies du centre-est de la Floride constitue un habitat pour plusieurs espèces menacées et en voie de disparition comme le geai à gorge blanche (*Aphelocoma coerulescens*). Des relevés précis d'occurrence d'incendies sont d'une importance capitale pour une meilleure connaissance de la relation entre les incendies et la structure de la végétation. Les taux de croissance rapides de la végétation adaptée aux incendies dans le centre-est de la Floride rendent difficile la détection précise des cicatrices d'incendie à l'aide de données de télédétection acquises plusieurs semaines après les incendies. L'objectif de cette étude est de développer une approche fiable basée sur la télédétection pour la cartographie précise des zones brûlées dans la végétation arbustive de Floride, dans la région du Centre spatial John F. Kennedy (KSC) de la National Aeronautics and Space Administration (NASA) et de la réserve faunique de Merritt Island National Wildlife Refuge (MINWR). Les données TM de Landsat, acquises le 21 avril 1987, ont été utilisées pour des expériences de classification. Les couches de données du système d'information géographique (SIG) des unités de gestion d'incendies (FMU) avec des éclosions documentées d'incendie (présence ou absence) ont été utilisées pour masquer les données originales de télédétection ou les cartes thématiques résultant de la classification. Un indice de séparation (IS) a été utilisé pour évaluer chaque bande individuelle pour sa capacité à discriminer les zones non brûlées des zones brûlées. Douze classifications utilisant des groupes de bandes spécifiques dérivés des données TM de Landsat représentant des étendues géographiques différentes ont été comparées à l'aide d'une matrice d'erreurs. La classification des quatre bandes les plus appropriées dérivées pour la zone entière de KSC–MINWR a donné la meilleure précision. Le produit cartographique final a été généré en superposant la carte classifiée et la couche de données des FMU et en masquant les FMU qui n'ont pas connu d'éclosion d'incendie. Cet article s'intéresse à plusieurs sujets reliés à la classification des zones brûlées incluant : l'effet de l'étendue géographique (effet EG) des données de télédétection sur la classification, la détermination des meilleures bandes pour la classification et l'épuration des résultats de classification à l'aide d'un masquage dans un SIG. Cet article constitue également le premier effort publié sur la cartographie des cicatrices d'incendie dans les communautés de végétation arbustive et de bas-fonds de Floride, dans le sud-est des Etats-Unis, basé sur l'utilisation des techniques de traitement d'images.
[Traduit par la Rédaction]

Received 19 February 2007. Accepted 30 May 2007. Published on the *Canadian Journal of Remote Sensing* Web site at http://pubs.nrc-cnrc.gc.ca/cjrs on 21 August 2007.

**G. Shao.**[1] Department of Forestry and Natural Resources, Purdue University, 715 West State Street, West Lafayette, IN 47907, USA.

**B.W. Duncan.** Dynamac Corporation, Mail Code DYN-2, Kennedy Space Center, FL 32899, USA; and Department of Biology, University of Central Florida, Orlando, FL 32816-2368, USA.

[1]Corresponding author (e-mail: shao@purdue.edu).

 

## Introduction

Fire is an important ecological factor maintaining vegetation in east-central Florida (Abrahamson and Hartnet, 1990; Myers, 1990; Duncan and Schmalzer, 2004). The historic natural fire regime of this region consisted of frequent spring and summer fires ignited by lightning (Duncan and Schmalzer, 2004). The fire regime of an area is defined by fire type (ground versus crown), intensity, size, return interval, seasonality, and spatial pattern. Native vegetation and many animal populations of this region are dependent on this fire regime (Stout, 2001). An example of a fire-dependent species in this region is the Florida scrub-jay (*Aphelocoma coerulescens*). The Florida scrub-jay is a threatened species that nests in oak scrub vegetation that resprouts after fire (Bowman and Woolfenden, 2002). Florida scrub-jay demography has been observed to peak in oak scrub habitat with optimum structure (120–170 cm tall scrub with scattered sand openings and little to no overstory) maintained by fire (Breininger and Carter, 2003). The recovery rate of oak scrub is highly variable and can take as few as 4 years or as many as 12 years to reach 120 cm tall after a fire occurs. If there is no fire for 15 years or greater, the oak scrub vegetation structure will change from shrubs to a closed-canopy forest, becoming unsuitable for most native fire-dependent species (Schmalzer, 2003).

The National Aeronautics and Space Administration (NASA) began acquiring land in early 1962 on Merritt Island, along the east coast of central Florida, where the John F. Kennedy Space Center (KSC) is located (**Figure 1**). A 57 000 ha area is managed primarily by the US Fish and Wildlife Service as the Merritt Island National Wildlife Refuge (MINWR). After NASA acquired the land, fire suppression went into effect on KSC until 1981. Fire suppression activity in the area combined with other anthropogenic influences (vegetation removal by facilities, roads, citrus farming, etc.) has altered vegetation structure, composition, and pattern on the landscape, reducing habitat for many plant and animal species. For example, the Florida scrub-jay population has experienced a dramatic decline throughout KSC–MINWR (Breininger et al., 1996). Restoration of the native vegetation structure using prescribed fire began in 1981, and then mechanical treatment techniques were added in 1992 and have become the major focus for natural resource management at KSC–MINWR (Schmalzer and Hinkle, 1992; Duncan et al., 1999; Duncan and Schmalzer, 2004). Breininger et al. (2002) suggested that understanding spatial variations in fire frequencies among vegetation types is important for sustaining suitable habitat structure for specialized plants and animals. Vegetation at KSC–MINWR has been burned by prescribed fires since 1981 at 3–12 year intervals depending on vegetation types. Documented fire records exist of all fires on KSC–MINW, including fire date, fire management units (FMUs), and estimated area burned, but no detailed fire scar pattern maps or area information are available. Optimization of fire management on KSC–MINWR for fire-dependent native

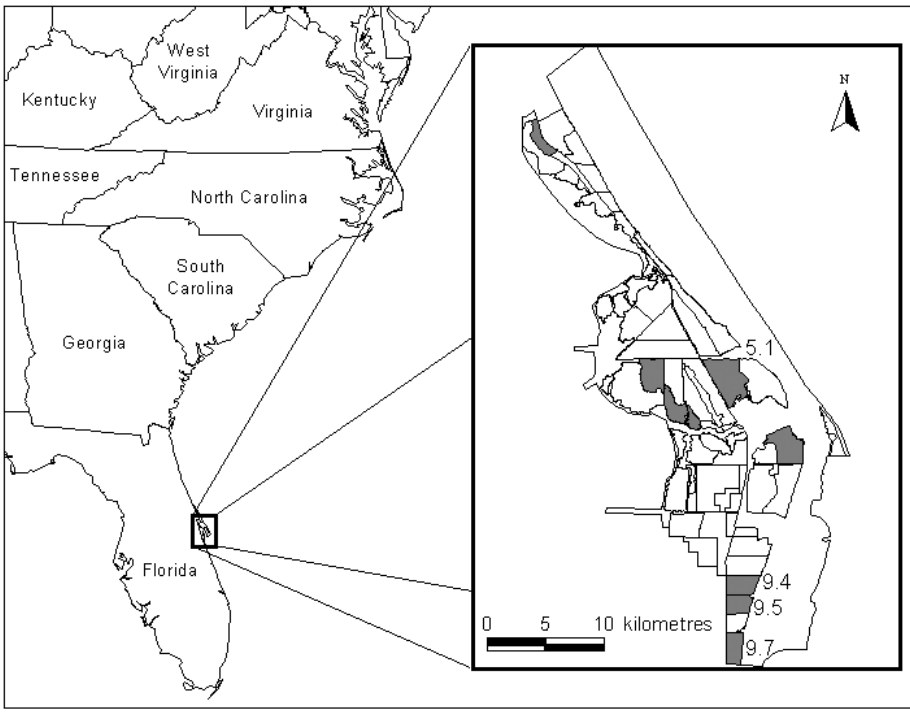


**Figure 1.** The location of NASA Kennedy Space Center (KSC) and Merritt Island National Wildlife Refuge (MINWR) in east-central Florida, USA. Relevant fire management units (FMUs) are indicated. The eight shaded FMUs were burned in 1986–1987 and were used for masking; the four labeled four FMUs (5.1, 9.4, 9.5, and 9.7) were used for band selection and accuracy assessment.

species requires that accurate spatial fire history records exist, including time since last burn and fire frequency information.

During the past two decades remote sensing has been used to identify and map fire scars in natural vegetation all around the world (Boyd and Danson, 2005). However, the remote sensing techniques used depend on the scale required for mapping. Eva and Lambin (1998) suggest that the most reliable strategy for estimating the extent of fire scars is through the use of a multisensor approach in which estimates of burned area acquired from low spatial resolution data are calibrated with high spatial resolution data. Before the year 2000, the main low-resolution sensor employed in continental- to global-scale fire-scar detection was the advanced very high resolution radiometer (AVHRR) on board the National Oceanic and Atmospheric Administration (NOAA) polar-orbiting platforms (Fuller, 2000; Maggi and Stroppiana, 2002). Recently, additional low spatial resolution remote sensing data from Système pour l'Observation de la Terre (SPOT) and moderate-resolution imaging spectroradiometer (MODIS) are available for fire-scar mapping (e.g., Amiro and Chen, 2003; Tansey et al., 2004; Csiszar et al., 2005). These sensors have multiple spectral bands, but only a subset of these bands (and (or) newly transformed bands) is used for fire-scar mapping. A study by Boschetti et al. (2004) that involved a comparison of three fire-scar datasets derived from low-resolution data showed major disagreements in terms of areal estimates. This suggests that fire-scar mapping using low-resolution remote sensing data needs further improvement.

Landsat data have been broadly employed for fire-scar mapping at both regional and local scales (e.g., Ranson et al., 2003; Hudak and Brockett, 2004; Mitri and Gitas, 2004; Pu and Gong, 2004). However, further study is required to determine how to use data characterized by low spectral resolution and what wavelengths (bands) are best for mapping fire scars. Pereira and Setzer (1993) found that thematic mapper (TM) channel 4 was the best for identifying fire scars, followed by channels 5, 3, and 7. Pu and Gong (2004) suggested that TM bands 4 and 7, the normalized difference vegetation index (NDVI) derived from TM4 and TM7, and the NDVI derived from TM bands 4 and 3 provided the best discrimination between burned scars and areas of unburned vegetation. Hudak and Brockett (2004) compared the tasseled cap (TC) and principal components (PC) transformations for mapping fire scars and found that PC helped differentiate the spectral signal of fire scars in each image. Patterson and Yool (1998) pointed out that bands transformed using the TC transformation resulted in a 17% higher overall classification accuracy than bands produced for the PC transform. Past studies, either at small or large scales, suggest that the usefulness of individual bands for fire-scar mapping depends on the data source (sensor), fire intensity, fire extent, and vegetation types. Less research has focused on studying the effects of varying geographic extents of remote sensing data on band selection and classification accuracy. In previous studies, classification accuracy has been used to evaluate how useful individual bands are for mapping fire scars (e.g., Pu and Gong, 2004); however, it is time consuming to perform classification experiments with every possible band combination from multispectral imagery.

Remotely sensed data are often integrated with geographic information systems (GIS) as part of the fire-scar mapping process (Chuvieco and Congalton, 1989). A GIS can be used to provide various ancillary data to enhance and validate image data classification (Sunar and Ozkan, 2001). High-quality remote sensing data are most frequently available in spring, relative to other seasons at KSC–MINWR. This is because spring is the driest season in this region and is typified by relatively long periods of cloud-free skies without storms.

The purpose of this paper is to compare various masking–classification options using Landsat TM data in concert with FMUs linked with existing KSC–MINWR fire records. As an initial effort in mapping fire scars for fire-adapted vegetation in east-central Florida, a classification experiment was conducted to provide information on a number of relevant issues related to the mapping and classification of fire scars using remotely sensed data. These include (*i*) the effect of geographic extents of remote sensing data on classification accuracy, (*ii*) detection of the best and optimum number of bands (or derived bands) for classification, and (*iii*) removing classification noise with GIS masking. The results from studying these issues will be useful for fire-scar mapping world wide and will be especially important for future fire mapping efforts in Florida and the southeast USA where reliable methods for mapping fires at this landscape scale (1 : 24 000 – 1 : 50 000) are not available.

## Methods

The data used for conducting the classification experiment included GIS data layers of the KSC boundary, FMUs, historical fire records associated with FMUs, and Landsat channel 5 TM data, path 16 and row 40, acquired on 21 April 1987. The TM dataset was rectified in State Plane coordinates in metres to make it spatially compatible with the GIS data layers. For safe management of fires, KSC–MINWR has been divided into 61 FMUs. These FMUs are of different sizes and shapes and are separated by nonflammable fire lines so that managed fires can be contained within selected areas. The FMUs are named using a numbering system with the first digit being a regional designator and the second digit after the decimal being a subunit within that region. Some of the units are further subdivided using letter designators such as A, B, and C. Based on the historical fire records, eight FMUs were partially burned with controlled fires between October 1986 and April 1987 (**Figure 1**). Fire scars at only four FMUs were previously digitized, and those at FMU9.4 were published (Breininger et al., 2002). Fire-scar data for FMU9.4 were used for sorting and selecting individual bands, and those for the other three FMUs (FMU5.1, FMU9.5, FMU9.7) were used to compute classification accuracy (**Figure 2**). Two different masking routines were tested and described to maximize classification accuracy.

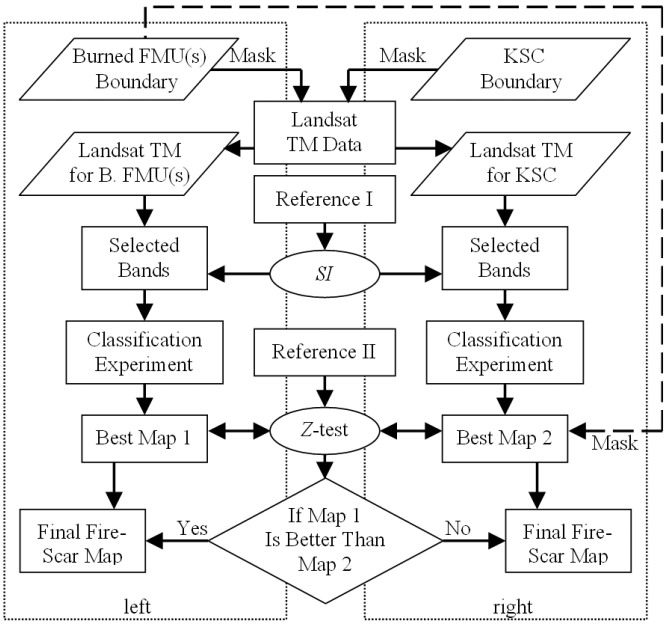


**Figure 2.** Work flow diagram of stepwise image processing for mapping fire scars at KSC–MINWR with Landsat TM data.

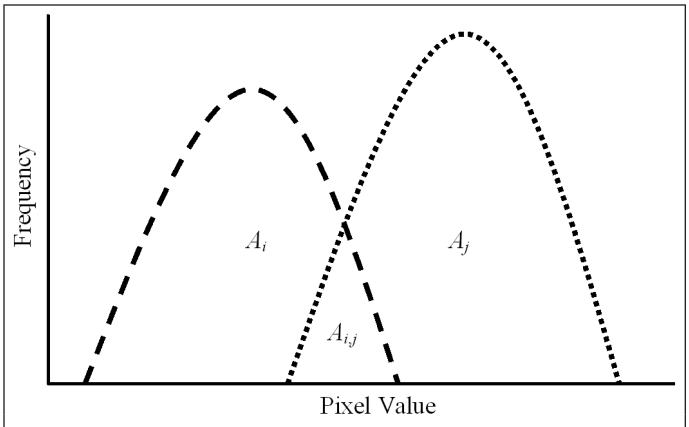


**Figure 3.** Illustration of the overlap of two histograms. Type *i* (dashed line) and type *j* (dotted line) can represent burned and unburned cover types. $A_{i,j}$ represents the overlap areas between burned and unburned cover types. $A_i$ and $A_j$ represent the area for burned and unburned cover types, respectively.

### Geographic extent determination by GIS masking

The rectified TM dataset was masked with the KSC–MINWR boundary (**Figure 2**, right) and with eight burned FMUs (**Figure 2**, left). The resultant image datasets are called KSC TM data and burned-FMU data. The NDVI between TM bands 4 and 3, PC transformation, and TC transformation were computed from KSC TM data and burned-FMU data, respectively. Rather than compress to eight bits, the original values of the transformed bands were used for classification.

To determine the association of how much information is in each TM band and each principal component, the correlation of each TM band $k$ with each PC $p$ was computed using the following formula (Jensen, 2004):

$$R_{kp} = \frac{a_{kp}\sqrt{\lambda_p}}{\sqrt{\mathrm{var}_k}} \quad (1)$$

where $a_{kp}$ is the eigenvector for bank $k$ and component $p$, $\lambda_p$ is the $p$th eigenvalue, and $\mathrm{var}_k$ is the variance of band $k$ in the covariance matrix.

### Band selection

The overlap area of histograms between burned and unburned areas was used to evaluate the potential of every band to separate burned and unburned areas. The new transformed bands and the original TM bands were overlaid with FMU9.4 fire-scar data. FMU9.4 was the only one used here, so the others (FMU5.1, FMU9.6, and FMU9.7) would be available later for accuracy assessment. Histograms of pixels values for each band were computed for burned and unburned areas (**Figure 3**). To avoid bias caused by the land cover type with larger area, the overlay area was divided by the area of a smaller land cover type. A simple index is calculated as follows:

$$\mathrm{SI}_{i,j} = 1 - \frac{A_{i,j}}{\min(A_i, A_j)} \quad (2)$$

where $\mathrm{SI}_{i,j}$ is the separation index between cover types $i$ and $j$ ($0 \le \mathrm{SI}_{i,j} \le 1$), $A_{i,j}$ is the overlap area between cover types $i$ and $j$, $A_i$ or $A_j$ is the area for cover type $i$ or $j$, and min represents the minimum function (using a smaller number between $A_i$ and $A_j$).

The higher the $\mathrm{SI}_{i,j}$ value, the more discriminative power the band has to separate the two cover types. All the bands with an $\mathrm{SI}_{i,j}$ value >0.1 were accepted for classification. Bands with $\mathrm{SI}i,j$ values >0.5 were called the most suitable bands and were stacked into a single image.

### Classification and assessment

For each TM dataset, original TM data, NDVI, selected PC bands, selected TC bands, the total of these bands, and the most suitable bands were used independently for classification. The unsupervised classification algorithm ISODATA was employed. The number of spectral classes was 20, the number of iterations was 20, and the convergence threshold was 0.99 for all the classifications with different band combinations. The 20 spectral classes were then manually recoded into two information classes, namely burned and unburned, to form the classified fire-scar maps. For each classification, an error matrix table was formed by overlaying the classification map with the digitized map from FMU5.1, FMU9.6, and FMU9.7. There were a total of 17 800 pixels in the three FMUs. Producer's accuracy and user's accuracy for burned-area cover type were computed. The mean accuracy value between producer's and user's accuracy was computed for each

classification. Fire-scar maps created with different bands were quantitatively compared with a *Z* test based on the error matrix tables (Congalton and Green, 1999). All the image data analyses were performed with Erdas Imagine (www.leica.com).

### Postclassification cleaning

Following each classification with the KSC TM dataset, the fire-scar maps were masked with a GIS data layer of the eight burned FMUs (**Figure 2**). This masking process, called postclassification cleaning, took advantage of the MINWR fire records and masked out any unburned FMUs. This step removed commission errors outside burned FMUs and assured a noise-free fire-scar map. When the burned-FMU TM dataset was used for classification, no further masking was needed for the fire-scar maps from the burned-FMU data. This was because the FMUs already represented the finest masking unit in this study.

## Results

### Geographic extent

*KSC TM data*

Among all the 15 bands, including seven original TM, one NDVI, four PC, and three TC bands, the bands with $SI_{i,j}$ values >0.5 were PC4, TM4, TC2, and NDVI (**Figure 4**). The first four PC bands had $SI_{i,j}$ values >0.1. Among the four PC bands, PC4 had the highest $SI_{i,j}$ value (**Figure 4b**). The eigenvalues for the four PCs were 8538.5, 696.1, 118.8, and 45.5 (**Table 1**), and they contained 99.9% of the total data variance. PC1 seemed correlated with every TM band, PC2 was only correlated with the near- and middle-infrared bands, and the other PCs were not correlated with any TM bands (**Table 1**).

*Burned-FMU data*

Among all the 14 bands, including seven original TM, one NDVI, three PC, and three TC bands, the bands with $SI_{i,j}$ values >0.5 were TM4, TC2, NDVI, and PC3 (**Figure 4**). The first three PC bands had $SI_{i,j}$ values >0.1. Among the three PC bands, PC3 had the highest $SI_{i,j}$ value (**Figure 4b**). The eigenvalues for the three PCs were 585.4, 365.4, and 26.2 (**Table 2**), and they contained 96.6% of the total data variance. PC1 seemed correlated with every TM band except for the thermal-infrared band; PC2 was only correlated with the near-, middle-, and thermal-infrared bands; PC3 was correlated with the visible bands, PC4 was correlated with the thermal-infrared band; and the other PCs were not correlated with any TM band (**Table 2**).

### Band selection

TM4 had the highest $SI_{i,j}$ value among the seven original TM bands, followed by TM2, TM6, and TM7 (**Figure 4a**). TM1, TM3, and TM5 had the lowest $SI_{i,j}$ values. The $SI_{i,j}$ value of NDVI was lower than that of TM4 but higher than those of other TM bands. Among the TC bands, TC2, a greenness band, had the highest $SI_{i,j}$ value, which was even higher than that of NDVI. TC1 (brightness) and TC3 (wetness) were less capable than TC2 at separating burned and unburned vegetation.

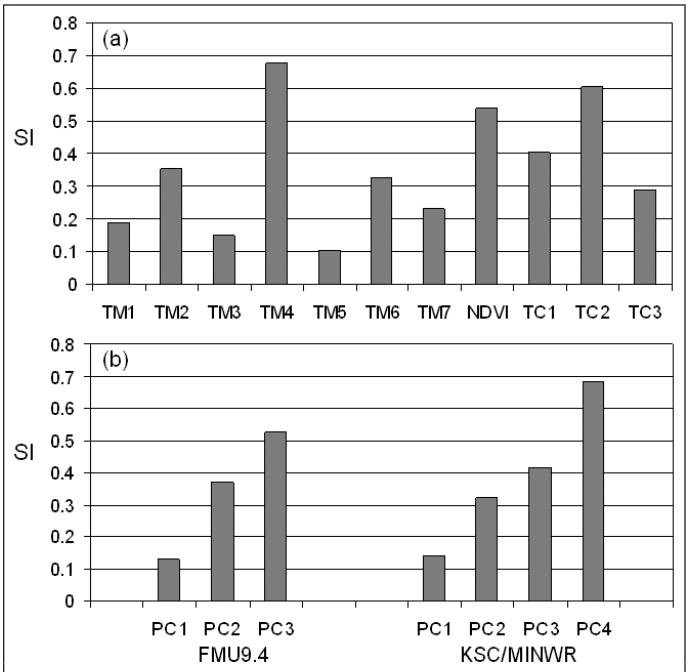


**Figure 4.** Comparison of $SI_{i,j}$ values: (a) seven original TM bands (TM1–TM7), one NDVI band, and three TC bands (TC1–TC3) common to both FMU9.4 and KSC–MINWR area; (b) three PC bands (PC1–PC3) for FMU9.4 and four PC bands (PC1–PC4) for KSC–MINWR area.

### Classification accuracy

When the KSC TM dataset was used for classification, the mean of producer's and user's accuracies for the burned cover class was 96.5% for the four most suitable bands (PC4, TM4, TC2, and NDVI), which was higher than that for three TC bands (94.3%), the original seven TM bands (93.9%), four PC bands (93.2%), NDVI (93.2%), and all 15 bands (91.6%) (**Figure 5a**). When the lower value between the producer's and user's accuracies was used for comparisons, the differences in classification accuracy among the six classifications were even greater: 95.8% for the four most suitable bands, 93.0% for the original seven TM bands, 92.2% for the four PC bands, 90.8% for the three TC bands, and 90.6% for all 15 bands. The *Z* test suggests that the classification map created with the four most suitable bands was significantly more accurate than those created with any of the other band combinations at a 99% confidence level (**Table 3**). The maps created with seven TM, four PC, and three TC bands had a significantly higher accuracy than those created with NDVI alone and all 15 bands.

When the burned-FMU TM dataset was used for classification, the original seven TM bands, one NDVI band, three PC bands, three TC bands, all 14 bands, and the four most suitable bands (TM4, TC2, NDVI, and PC3) resulted in a mean accuracy ranging from 91.2% to 93.8% for the burned cover

**Table 1.** Relationship of the original TM bands to the principal components (PC) from the KSC TM dataset.

| Original | PC | | | | | | |
|---|---|---|---|---|---|---|---|
| TM band | 1 | 2 | 3 | 4 | 5 | 6 | 7 |
| 1 | 0.8110 | –0.1257 | 0.0680 | –0.0475 | 0.0178 | –0.0014 | –0.0037 |
| 2 | 0.9825 | –0.0789 | 0.1254 | –0.1076 | –0.0040 | 0.0020 | 0.0329 |
| 3 | 0.9675 | 0.0356 | 0.2179 | –0.0948 | –0.0772 | 0.0150 | –0.0090 |
| 4 | 0.8812 | 0.4070 | –0.2135 | –0.1100 | –0.0037 | –0.0104 | –0.0012 |
| 5 | 0.8320 | 0.5447 | 0.0783 | 0.0653 | 0.0120 | 0.0232 | 0.0005 |
| 6 | 0.9712 | –0.1434 | –0.0569 | 0.0507 | –0.0056 | 0.0000 | 0.0006 |
| 7 | 0.7828 | 0.5412 | 0.2659 | 0.1223 | –0.0092 | –0.0924 | 0.0005 |
| Eigenvalue | 8538.5 | 696.1 | 118.8 | 45.5 | 3.7 | 2.6 | 0.5 |

**Table 2.** Relationship of the original TM bands to the PCs from the burned-FMU TM dataset.

| Original | PC | | | | | | |
|---|---|---|---|---|---|---|---|
| TM band | 1 | 2 | 3 | 4 | 5 | 6 | 7 |
| 1 | 0.8167 | –0.1424 | –0.5228 | 0.1527 | –0.0200 | –0.1309 | 0.0184 |
| 2 | 0.8592 | 0.1993 | –0.4135 | 0.1279 | –0.0488 | 0.0536 | –0.1757 |
| 3 | 0.8767 | –0.1209 | –0.4290 | 0.0542 | –0.1108 | 0.1246 | 0.0504 |
| 4 | 0.5314 | 0.8338 | 0.0474 | 0.1240 | 0.0279 | 0.0023 | 0.0035 |
| 5 | 0.9795 | –0.1474 | 0.0848 | –0.0961 | –0.0493 | –0.0075 | –0.0013 |
| 6 | –0.0100 | –0.8712 | 0.1688 | 0.4436 | –0.0979 | –0.0012 | –0.0008 |
| 7 | 0.7108 | –0.6831 | –0.0056 | 0.0468 | 0.1526 | 0.0124 | 0.0010 |
| Eigenvalue | 585.4 | 363.4 | 26.2 | 25.7 | 6.3 | 1.4 | 0.6 |

type (**Figure 5b**). Band NDVI alone resulted in the lowest mean accuracy. If the lower value between producer's and user's accuracy was used for comparison, the classification with the four most suitable bands had a relatively high accuracy of 93.7%, which is better than that of classifications with other bands, whose accuracies were 92.2%, 92.1%, 91.2%, 91.1%, and 89.4% for the original seven TM, three PC, three TC, NDVI, and all 14 bands, respectively. By comparing $Z$ values at the 99% confidence level, all six classification maps were grouped into three accuracy levels: the highest accuracy group contained maps created with seven TM, three PC, and the four most suitable bands; the lowest accuracy group contained maps created with NDVI and all 14 bands; and the map created with three TC bands had an accuracy in the middle between those of the lowest and highest accuracy groups (**Table 4**).

When all the accuracy statistics were considered, the classifications with both TM datasets had a similar trend in classification accuracy: the four most suitable bands resulted in the best maps, and NDVI and the stack of all the bands resulted in the worst classifications; the fire-scar maps created with the four most suitable bands had low variation between producer's and user's accuracies; and both fire-scar maps created with the original seven TM, three PC, or three TC bands had similar combinations of producer's and user's accuracy. The classification with the KSC TM dataset was generally superior to that with the burned-FMU TM dataset. The $Z$ value between the two maps created with the four most suitable bands derived from image data for KSC and burned FMUs was 15.83, which is much higher than the critical $Z$ value of 2.58 at a 99% confidence level.

### Postclassification cleaning

Because the four most suitable bands derived from the KSC TM dataset resulted in a higher classification accuracy than those derived from the burned-FMU TM dataset, the procedure described in the right-hand column of **Figure 2** was the better choice. In this case, the four most suitable bands derived from the KSC TM dataset were chosen for final classification. The immediate result of image data classification with the four most suitable bands contained information about old fire scars and misclassification noise in other FMUs. To reduce noise in the fire-scar map, the resultant classification map was masked with a GIS data layer of the eight burned FMUs (**Figure 6**).

## Discussion

### Effects of geographic extent

In addition to the significant increase in classification accuracy by using the four most suitable bands for both TM datasets, there was another slight increase in classification accuracy when the TM imagery was masked with the burned FMUs (**Figure 5**). This may have to do with the fact that burned FMUs were so small in area that the local variability of the TM data could not represent the global variability of typical cover classes. A difference in geographic extent of the TM data also

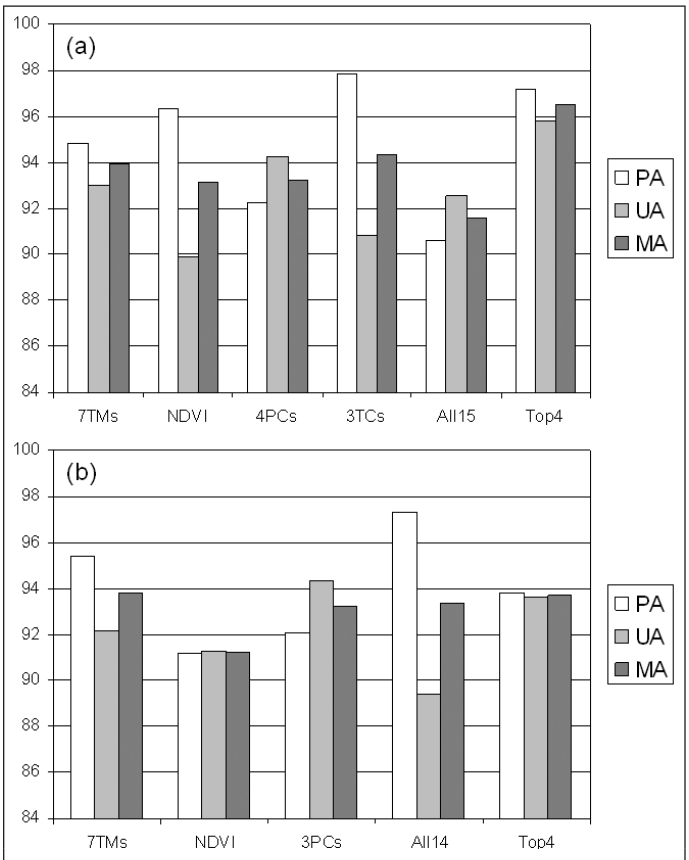


**Figure 5.** A comparison in classification accuracy among different band combinations derived from (a) the KSC TM dataset and (b) the burned-FMU TM dataset. MA, mean of producer's accuracy and user's accuracy; PA, producer's accuracy; UA, user's accuracy.

affects transformed PC bands. From this point of view, geographic extent of remote sensing data cannot be overlooked in image data classification.

The most effective PC bands for fire-scar mapping were not those with the highest or lowest eigenvalues. In other words, the PC band with a relatively low eigenvalue was powerful in discriminating burned from unburned areas. This is because fire scars were local phenomena, and spectral variance between burned and unburned cover types in the study area accounted for a small fraction of the total data variance and did not enter the earlier components. The covariance matrix used to generate PCs is a global variability measure of the original image segment, and local variability may appear in a later component (Richards, 1986). This was exactly what happened when mapping fire scars with PC bands in this study. Because of the differences in geographic extent between the FMU and KSC TM datasets, the PCs that capture the variance between burned and unburned areas did not necessarily stay in the same order. The geographic extent of remote sensing data and its influence on band selection and classification accuracy may explain the band selection variation of past studies, as they were conducted at different spatial scales.

## Band selection

Fire scars in the fire-adapted vegetation at KSC–MINWR are relatively small in terms of geographic extent, but their spatial variation determines habitat suitability for the Florida scrub-jay (Breininger et al., 1998). Time since fire influences vegetation height, and the pattern of fire determines the mosaic pattern of vegetation heights, influencing Florida scrub-jay demography (Breininger and Carter, 2003). Minor vegetation changes can alter habitat conditions for threatened and endangered animals and plants (Schmalzer, 2003). The sensitive nature of the habitat demands a high standard for mapping fire scars at KSC–MINWR. We chose to use Landsat TM data because they are available since the mid-1980s and have suitable spatial and spectral resolution. We examined several groups of spectral bands to obtain the optimal classification. This was a different approach from fire-scar mapping with NDVI alone (e.g., Salvador et al., 2000) or with all the PC bands (e.g., Hudak and Brockett, 2004). Our experiment suggests that too few bands (e.g., NDVI alone) or too many bands (e.g., a total of 14 or 15 bands) were not optimal for mapping fire scars at KSC–MINWR.

Comparing individual bands and their capabilities for identifying fire scars was an effective approach for band selection (e.g., Pereira and Setzer, 1993; Pu and Gong, 2004). Classification accuracy has been used for evaluating individual bands, but image data classification is a time-consuming process. Unlike other statistical methods of feature selection, such as transformed-divergence (Jensen, 2004), which are used to measure how close two signatures are for different band combinations in supervised classification, the separation index or $SI_{i,j}$ in this study is a nonparametric measure for exclusively examining how effective each individual band is for separating two classes. In discriminating burned and unburned areas, the $SI_{i,j}$ proved convenient and dependable for band comparisons. Our results suggest that bands with high $SI_{i,j}$ values, when combined, can result in relatively high classification accuracy. This quantitative method may have a general applicability for mapping fire scars with remotely sensed data.

It is not surprising that TM4, NDVI, and TC2 are capable of separating burned and unburned areas because they all reflect the greenness of land surface. Although these three bands are correlated, they do not completely represent each other. Because the selected PC bands were not correlated with TM4 (**Tables 1, 2**), their roles in increasing classification accuracy may be more important than those of any other individual green bands.

## Classification assessment

A number of accuracy statistics or measures can be derived from error matrices (Congalton and Green, 1999), but each has unique implications (Foody, 2002). The mean accuracy in this study has a meaning similar to that of the individual classification success index proposed by Koukoulas and Blackburn (2001). Normally the difference between user and producer accuracy for a cover type has a close relationship with the area to be estimated for that type (Shao et al., 2003).

**Table 3.** *Z* values based on error matrix tables between different classification maps created with spectral bands derived from the KSC TM dataset.

| | NDVI | Four PC bands | Three TC bands | All 15 bands | Four most suitable bands |
|---|---|---|---|---|---|
| Seven TM bands | 7.21* | 1.08 | 2.02 | 8.86* | 15.03* |
| NDVI | | 6.24* | 5.12* | 1.39 | 21.88* |
| Four PC bands | | | 0.98 | 16.38* | 7.87* |
| Three TC bands | | | | 6.67* | 16.73* |
| All 15 bands | | | | | 24.15* |

*Significant difference at the 99% confidence level.

**Table 4.** *Z* values based on error matrix tables between different maps created with spectral bands derived from burned-FMU TM dataset.

| | NDVI | Three PC bands | Three TC bands | All 14 bands | Four most suitable bands |
|---|---|---|---|---|---|
| Seven TM bands | 9.13* | 0.78 | 2.72* | 6.66* | 1.85 |
| NDVI | | 10.09* | 6.33* | 2.26 | 11.10* |
| Three PC bands | | | 3.54* | 7.54* | 1.11 |
| Three TC bands | | | | 3.94* | 4.59* |
| All 14 bands | | | | | 8.54* |

*Significant difference at the 99% confidence level.

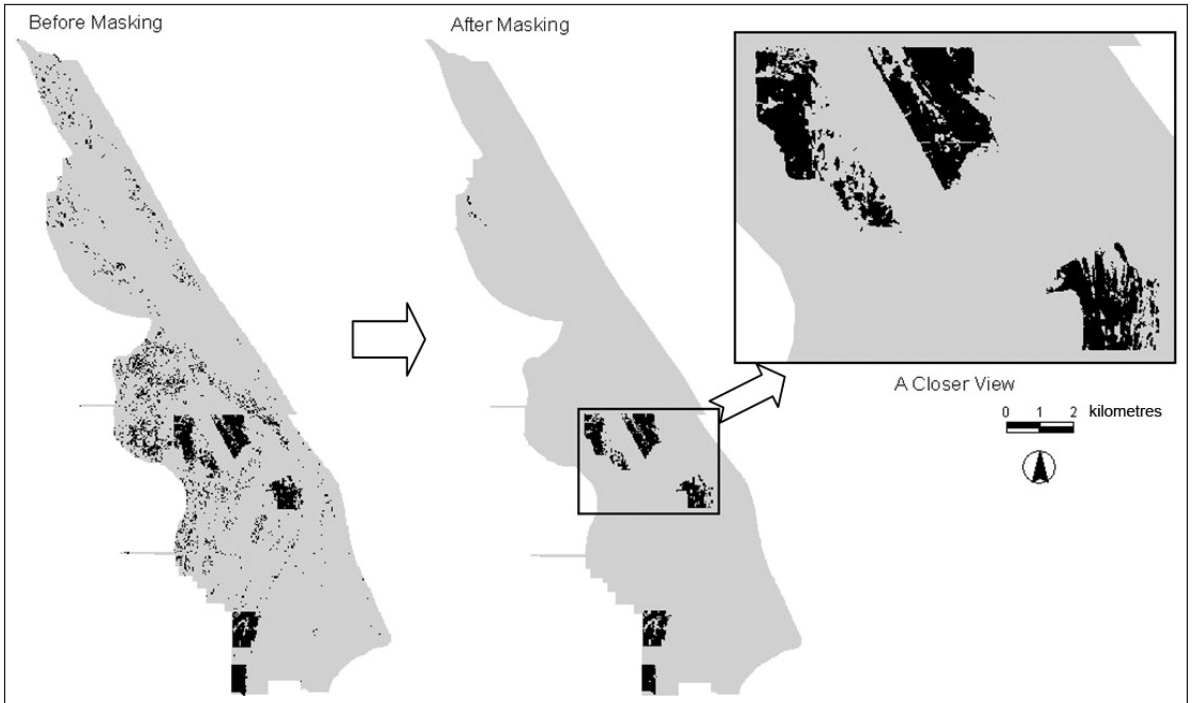


**Figure 6.** The reduction of classification noise through GIS masking. A comparison of before and after GIS masking, with fire scars shown in black. Fire scars were classified using PC4, TM4, TC2, and NDVI derived from the KSC TM dataset.

Classifications with the same mean accuracy but with a large difference between user and producer accuracy have different implications in terms of area estimation accuracy for a given cover type. Because the *Z* test uses all the numbers of an error matrix, it indirectly considers the variations of user and producer accuracy. For example, the fire-scar map created with three TC bands derived from the burned-FMU TM dataset was significantly different from different maps created with other band combinations, though its mean accuracy value was close to those of the other maps (**Figure 5a**). An ideal fire-scar map should have a high mean accuracy but a low difference between user and producer accuracy. This explains how the fire-scar map based on the four most suitable bands derived from the burned-FMU TM dataset was superior to other maps in the FMU masking experiment (**Figure 5a**). The fire-scar map based on the four most suitable bands derived from the KSC

TM dataset was indeed the best choice because it had the highest mean accuracy and relatively low difference between user accuracy and producer accuracy (**Figure 5b**). Since both fire-scar maps based on the four most suitable bands were better than those based on other bands, the combination of the most suitable bands seemed reliable in enhancing the accuracy of the fire-scar mapping, even if they were correlated.

## Summary and conclusions

Both band combination and the geographic extent of remote sensing data affect the quality of fire-scar maps produced. Therefore, a reliable image processing procedure for mapping fire scars at KSC must include four steps. Step one was to mask the TM data with the KSC boundary data layer. The resultant TM dataset contains information beyond burned areas. Step two was to use the separation index ($SI_{i,j}$) to evaluate each individual band for its potential capability in discriminating unburned and burned areas. By comparing and sorting all the bands of interest, it was possible to select reliable bands for image data classification. Step three was to compare classifications with selected band groups derived from Landsat TM data. This helped determine the best band combinations for discriminating unburned and burned areas. Step four was to clean the classification map by masking it with the burned FMUs GIS layer. This removed all the noise outside the burned FMUs and beyond the fire-detection period, resulting in an accurate fire-scar map.

There are many options for fire-scar mapping with geospatial data. Specific mapping techniques depend not only on sensor type, but also on vegetation type and fire properties (Eva and Lambin, 1998; Boyd and Danson, 2005). The comparison of various classification options in this study not only led to a reliable approach to detect detailed fire scars within the rapidly growing vegetation of this region, but also highlighted four general concerns: (*i*) the geographic extent of remote sensing data used for classification affects discriminative power of individual bands generated from the data and, therefore, cannot be overlooked for classification; (*ii*) many spectral bands can be derived from remote sensing data, but only a limited number of bands can lead to satisfactory results for a specific classification purpose, and eigenvalues should not solely be relied on for PC band selections; (*iii*) a classification based on too few or too many bands is a poor choice, and an optimum band combination depends on the discriminative capability of the individual bands, but not on the correlations among the bands; and (*iv*) GIS masking is an effective method of cleaning fire-scar maps. The GIS data layers can be obtained from ground records or with coarser resolution remote sensing data. Administrative regions, natural watersheds, or management units can be used as mask data.

This remote sensing technique will support both historic and future fire-scar mapping work on KSC–MINWR and potentially other locations in the southeastern United States and fire-dependent systems world wide. Fires in this region typically form complex mosaic patterns with enclaves of unburned fuels throughout the burned area, requiring inordinate amounts of effort to map by field survey. This remote sensing technique will provide a means to map future fire scars in an efficient and consistent manner. This technique is most readily transferable to areas with some existing fire records documenting the date and general location of past fires. Future work may strive to increase available information by documenting fire intensities and mixed pixel contributions by burned–unburned fractions. By advancing this technique further, it will become even more ecologically relevant when dealing with the habitat needs of specialized native fire-dependent species, increasing its utility for land managers.

## Acknowledgements

The research was supported by NASA Summer Faculty Research in the United States in 2005. The authors thank David Breininger for his assistance in data collection and analysis and Paul Schmalzer for his efforts in editing this paper. The associate editor and two reviewers provided constructive suggestions for improving the paper.

## References

Abrahamson, W.G., and Hartnett, D.C. 1990. Pine flatwoods and dry prairies In *Ecosystems of Florida*. Edited by R.L. Myers and J.J. Ewel. University of Central Florida Press, Orlando, Fla. pp. 103–149.

Amiro, B.D., and Chen, J.M. 2003. Forest-fire-scar aging using SPOT–VEGETATION for Canadian ecoregions. *Canadian Journal of Forest Research*, Vol. 33, No. 6, pp. 1116–1125.

Boschetti, L., Eva, H.D., Brivio, P.A., and Gregoire, J.M. 2004. Lessons to be learned from the comparison of three satellite-derived biomass burning products. *Geophysical Research Letters*, Vol. 31, Art. L21501.

Bowman, R., and Woolfenden, G.E. 2002. Nest site selection by Florida Scrub-Jays in natural and human-modified habitats. *Wilson Bulletin*, Vol. 114, No. 1, pp. 128–135.

Boyd, D.S., and Danson, F.M. 2005. Satellite remote sensing of forest resources: three decades of research development. *Progress in Physical Geography*, Vol. 29, No. 1, pp. 1–26.

Breininger, D.R., and Carter, G.M. 2003. Territory quality transitions and source-sink dynamics in a Florida Scrub-Jay population. *Ecological Applications*, Vol. 13, No. 2, pp. 516–529.

Breininger, D.R., Larson, V.L., Oddy, D.M., Smith, R.B., and Barkaszi, M.J. 1996. Florida Scrub-Jay demography in different landscapes. *Auk*, Vol. 113, No. 3, pp. 617–625.

Breininger, D.R., Larson, V.L., Duncan, B.W., and Smith, R.B. 1998. Linking habitat suitability to demographic success in Florida scrub-jays. *Wildlife Society Bulletin*, Vol. 26, No. 1, pp. 118–128.

Breininger, D.R., Duncan, B.W., and Dominy, N.J. 2002. Relationships between fire frequency and vegetation type in pine flatwoods of East-Central Florida, USA. *Natural Areas Journal*, Vol. 22, No. 3, pp. 186–193.

Chuvieco, E., and Congalton, R.G. 1989. Application of remote-sensing and geographic information-systems to forest fire hazard mapping. *Remote Sensing of Environment*, Vol. 29, No. 2, pp. 147–159.

Congalton, R.G., and Green, K. 1999. *Assessing the accuracy of remotely sensed data: principles and practices*. Lewis Publisher, New York.

Csiszar, I., Denis, L., Giglio, L., Justice, C.O., and Hewson, J. 2005. Global fire activity from two years of MODIS data. *International Journal of Wildland Fire*, Vol. 14, No. 2, pp. 117–130.

Duncan, B.W., and Schmalzer, P.A. 2004. Anthropogenic influences on potential fire spread in a pyrogenic ecosystem of Florida, USA. *Landscape Ecology*, Vol. 19, No. 2, pp. 153–165.

Duncan, B.W., Boyle, S., Breininger, D.R., and Schmalzer, P.A. 1999. Coupling past management practice and historic landscape change on John F. Kennedy Space Center, Florida. *Landscape Ecology*, Vol. 14, No. 3. pp. 291–309.

Eva, H., and Lambin, E.F. 1998. Remote sensing of biomass burning in tropical regions: sampling issues and multisensor approach. *Remote Sensing of Environment*, Vol. 64, No. 3, pp. 292–315.

Foody, G.M. 2002. Status of land cover classification accuracy assessment. *Remote Sensing of Environment*, Vol. 80, No. 1, pp. 185–201.

Fuller, D.O. 2000. Satellite remote sensing of biomass burning with optical and thermal sensors. *Progress in Physical Geography*, Vol. 24, No. 4, pp. 543–561.

Hudak, A.T., and Brockett, B.H. 2004. Mapping fire scars in a southern African savannah using Landsat imagery. *International Journal of Remote Sensing*, Vol. 25, No. 16, pp. 3231–3243.

Jensen, J.R. 2004. *Introductory digital image processing: a remote sensing perspective*. 3rd ed. Prentice Hall Inc., Upper Saddle River, N.J.

Koukoulas, S., and Blackburn, G.A. 2001. Introducing new indices for accuracy evaluation of classified images representing semi-natural woodland environments. *Photogrammetric Engineering & Remote Sensing*, Vol. 67, No. 4, pp. 499–510.

Maggi, M., and Stroppiana, D. 2002. Advantages and drawbacks of NOAA–AVHRR and SPOT–VGT for burnt area mapping in a tropical savanna ecosystem *Canadian Journal of Remote Sensing*, Vol. 28, No. 2, pp. 231–245.

Mitri, G.H., and Gitas, I.Z. 2004. A semi-automated object-oriented model for burned area mapping in the Mediterranean region using Landsat-TM imagery. *International Journal of Wildland Fire*, Vol. 13, No. 3, pp. 367–376.

Myers, R.L. 1990. Scrub and high pine. In *Ecosystems of Florida*. Edited by R.L. Myers and J.J. Ewel. University of Central Florida Press, Orlando, Fla. pp. 150–193.

Patterson, M.W., and Yool, S.R. 1998. Mapping fire-induced vegetation mortality using Landsat Thematic Mapper data: a comparison of linear transformation techniques. *Remote Sensing of Environment*, Vol. 65, No. 2, pp. 132–142.

Pereira, M.C., and Setzer, A.W. 1993. Spectral characteristics of fire scars in Landsat-5 TM images of Amazonia. *International Journal of Remote Sensing*, Vol. 14, No. 11, pp. 2061–2078.

Pu, R.L., and Gong, P. 2004. Determination of burnt scars using logistic regression and neural network techniques from a single post-fire Landsat 7 ETM+ image. *Photogrammetric Engineering & Remote Sensing*, Vol. 70, No. 7, pp. 841–850.

Ranson, K.J., Kovacs, K., Sun, G., and Kharuk, V.I. 2003. Disturbance recognition in the boreal forest using radar and Landsat-7. *Canadian Journal of Remote Sensing*, Vol. 29, No. 2, pp. 271–285.

Richards, A.J. 1986. *Remote sensing digital image analysis: an introduction*. Springer-Verlag, New York. pp. 137–138.

Salvador, R., Valeriano, J., Pons, X., and Diaz-Delgado, R. 2000. A semi-automatic methodology to detect fire scars in shrubs and evergreen forests with Landsat MSS time series. *International Journal of Remote Sensing*, Vol. 21, No. 4, pp. 655–671.

Schmalzer, P.A. 2003. Growth and recovery of oak saw palmetto scrub through ten years after fire. *Natural Areas Journal*, Vol. 23, No. 1, pp. 5–13.

Schmalzer, P.A., and Hinkle, C.R. 1992. Recovery of oak-saw palmetto scrub after fire. *Castanea*, Vol. 57, No. 1, pp. 158–173.

Shao, G.F., Wu, W.C., Wu, G., Zhou, X.H., and Wu, J.G. 2003. An explicit index for assessing the accuracy of cover class areas. *Photogrammetric Engineering & Remote Sensing*, Vol. 69, No. 8, pp. 907–913.

Stout, I.J. 2001. Rare plants of the Florida scrub, USA. *Natural Areas Journal*, Vol. 21, No. 1, pp. 50–60.

Sunar, F., and Ozkan, C. 2001. Forest fire analysis with remote sensing data. *International Journal of Remote Sensing*, Vol. 22, No. 12, pp. 2265–2277.

Tansey, K., Gregoire, J.M., Stroppiana, D., Sousa, A. Silva, J., Pereira, J.M.C., Boschetti, L., Maggi, M., Brivio, P.A., Fraser, R., Flasse, S., Ershov, D., Binaghi, E., Graetz, D., and Peduzzi, P. 2004. Vegetation burning in the year 2000: Global burned area estimates from SPOT VEGETATION data. *Journal of Geophysical Research-Atmospheres*, Vol. 109, Art. D14S03.